Strain-induced crystallization of natural rubber subjected to biaxial loading conditions as revealed by X-ray diffraction

Stéphanie Beurrot, Bertrand Huneau, Erwan Verron

Strain-induced crystallization of natural rubber subjected to biaxial loading conditions as revealed by X-ray diffraction

S. Beurrot, B. Huneau & E. Verron
LUNAM Université, Ecole Centrale de Nantes, GeM, UMR CNRS 6183
BP 92101, 44321 Nantes cedex 3, France

ABSTRACT: Strain induced crystallization (SIC) in carbon black-filled natural rubber (NR) is investigated by wide-angle X-ray diffraction (WAXD) using synchrotron radiation for three deformation states: uniaxial, biaxial (but non-equibiaxial) and equibiaxial tension. The crystallites size is of the same order of magnitude and the lattice parameters are similar for the three states. But the orientation of the crystallites varies: as the crystallites are highly oriented accordingly to the tensile direction for uniaxial loading condition, they are oriented (but with a higher degree of disorientation) along the tensile direction (highest stretch ratio) for biaxial loading condition, and they are not oriented in the plane of tension for equibiaxial loading condition.

1 INTRODUCTION

Natural rubber (NR), cis-1,4-polyisoprene, has remarkable mechanical properties which are generally explained by strain-induced crystallization (SIC). SIC is commonly investigated by wide-angle X-ray diffraction (WAXD) (see Murakami et al. 2002, Toki et al. 2002, Toki et al. 2003, Trabelsi et al. 2003a among others, for a more complete review of these works, the reader can refer to Huneau 2011). The great majority of the studies on SIC focuses on uniaxial tension; but as engineering applications involve multiaxial loading conditions, mechanical models must take into account the multiaxiality of the material response; for example, it is well-known that the efficiency of a given constitutive equation for rubber-like materials requires shear or biaxial experimental data (Marckmann and Verron 2006). In this way, the present paper is devoted to the experimental study of biaxial strain-induced crystallization of NR by X-ray diffraction using synchrotron radiation. To our knowledge, this is the second study on the influence of biaxiality on strain-induced crystallization of natural rubber: Oono et al. (1973) studied the orientation of crystallites in a stretched thin film of unfilled vulcanized natural rubber at -27°C.

Here, we compare *(i)* the orientation and *(ii)* the size of the crystallites, and *(iii)* the lattice parameters of the crystal unit cell in filled NR submitted to uniaxial, biaxial and equibiaxial loading conditions, at room temperature and for thick samples.

2 EXPERIMENTAL METHOD

2.1 *Material, sample and local strain measurement*

The material used in this study is a classic carbon black-filled natural rubber. The composition is given in Table 1.

Table 1: Chemical composition of the filled NR used in this study (g per 100 g of rubber).

rubber	100
carbon black (N330)	50
zinc oxyde	5
stearic acid	2
sulfur	1.2
accelerator (CBS)	1.2
antioxydant	1

Figure 1 shows the two samples used in this study. The uniaxial tensile tests were performed on classical flat dumbbell specimens; dimensions are given in Fig. 1a. Obtaining biaxial deformation for soft materials is not an easy task (Demmerle and Boehler 1993). For this study, we developed a cruciform sample, based on a symmetric cross thinned at its center as shown in Fig. 1b and 1c. Under loading, the arms of the sample are uniaxially stretched and the central zone is in a complex deformation state (see Fig. 1d). When the four arms are equally stretched, the only point at which the deformation is equibiaxial is the center point of the specimen. The central part of the sample is made thinner in order to reach higher strain levels, without breaking the arms of the cross sample. Both homogeneity and equibiaxiality were verified by finite element analysis and the zone in which

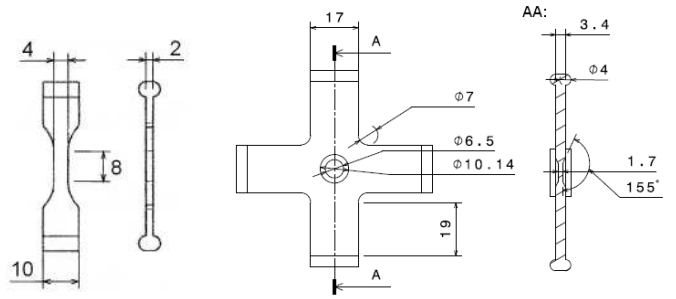

(a) (b)

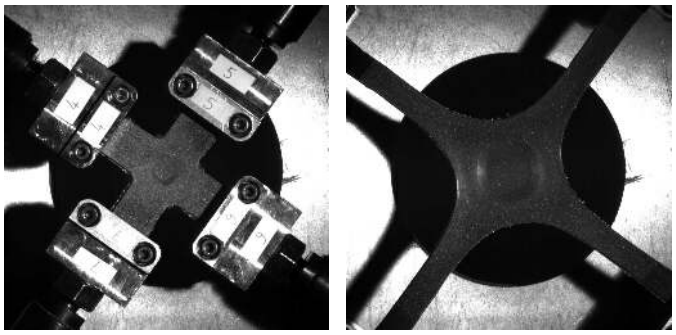

(c) (d)

Figure 1: Dimensions of the (a) uniaxial samples and (b) biaxial samples. Cruciform sample (c) in undeformed state and (d) in equibiaxial deformation state.

the material is subjected to nearly equibiaxial tension is quiet larger than the beam spot, i.e. about 3 mm^2. To achieve biaxial but non-equibiaxial deformation at the center of the sample, two opposite arms of the cross sample are simply more stretched than the two other ones.

As the cross sample is in a complex state of deformation when the arms are stretched, it is difficult to predict the stretch ratio in the center of the sample from the values of displacement of the actuators only. Therefore, the biaxial tests have been filmed and a motion analysis system (Tema motion©) has been used to track the displacement of points of a paint pattern applied at the center of the sample. It allowed to determine the deformation gradient **F** from which the two stretch ratios in the directions parallel to the plane of tension are extracted. The general form of the deformation gradient, assuming incompressibility, is :

$$\mathbf{F} = \begin{bmatrix} \lambda & 0 & 0 \\ 0 & \lambda^B & 0 \\ 0 & 0 & \lambda^{-B-1} \end{bmatrix} \quad (1)$$

where B is the biaxiality factor, $B \in [-0.5; 1]$. One can note that $B = -0.5$ for a material subjected to uniaxial tension and $B = 1$ in the case of equibiaxial tension. When the material is subjected to biaxial (non-equibiaxial) tension, $B \in]0; 1[$.

2.2 *Synchrotron*

Synchrotron measurements have been carried out at the DiffAbs beamline in the French national synchrotron facility SOLEIL. The wavelength used is 1.319 Å and the beam size is 0.3 mm in diameter at half-maximum. The 2D WAXD patterns are recorded by a MAR 345 CCD X-ray detector. In order to make an accurate correction of air scattering, a PIN-diode beam stop was used.

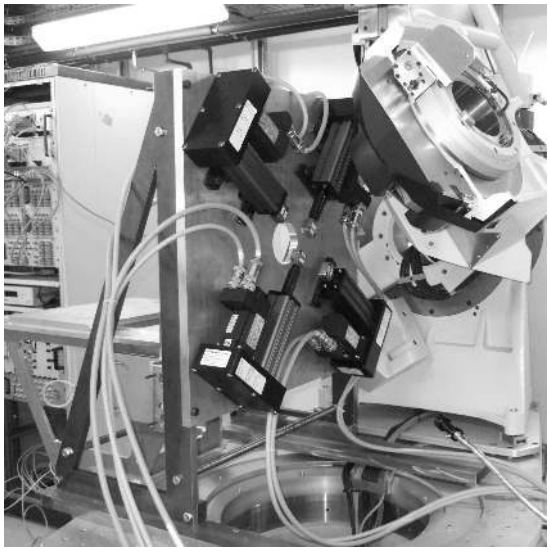

Figure 2: Uniaxial and biaxial stretching machine in DiffAbs.

2.3 *Tensile testing machine*

The experiments have been conducted with a homemade stretching machine shown in Figure 2. It is composed of four electrical actuators, which displacements can be synchronized or not. Their loading capacity is ± 500 N and their stroke is 75 mm each. All the experiments are conducted by prescribing the displacement of these actuators. Opposite actuators always have opposite equal displacements in order to keep the central zone of the sample fixed. For uniaxial tests, only two actuators are used; for biaxial tests, the four actuators are used.

2.4 *Procedure*

The stretching unit is placed on the stand of the diffractometer (see Fig. 2) in order to keep the beam focused on the centre of the samples. The uniaxial experiment is quasi-static (the actuators speed is set to 0.012 mm/s) and scattering patterns are recorded every 100 seconds (due to the reading time of the CCD detector). For the biaxial experiments, the actuators speed is 30 mm/s, and one pattern is recorded at maximum deformation. The exposure time is short (1 second for uniaxial test and 3 seconds for biaxial tests): it permits to reduce the influence of kinetics of crystallization on the results.

An air scattering pattern (without sample) was first collected and has been used to correct the patterns. Moreover, the change in thickness of the sample under extension and the change of intensity of the incident photons have also been considered. All these corrections are performed by following the well-established method of Ran et al. (2001). Both the determination of the pattern center and the calibration

of the diffraction angles were achieved by considering the first diffraction ring of ZnO ((100)-plane, $a = 3.25$ Å (Reeber 1970)). Here, small angles scattering is not investigated; the range of diffraction angles is $2\theta \in [8°, 26.7°]$.

2.5 *Scattering pattern analysis*

The spectra extracted from the diffraction patterns are classically fitted by series of Pearson functions (Trabelsi et al. 2003a, Chenal et al. 2007, Rault et al. 2006, Toki et al. 2000); before deconvolution, the linear baseline of each spectrum is suppressed (see example in Figure 3). The lattice parameters of the crystal cell

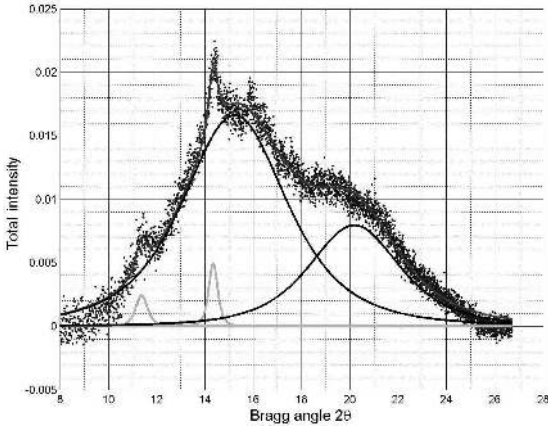

Figure 3: Example of fitting and deconvolution of a spectrum with a series of Pearson functions.

of the polyisoprene are calculated considering a monoclinic crystal system, as determined by Bunn (1942). The crystallites size is deduced from the Scherrer formula (Guinier 1963):

$$l_{hkl} = \frac{K\lambda}{\text{FWHM}_{2\theta}\cos\theta} \tag{2}$$

where l_{hkl} is the crystallites size in the direction normal to the hkl plane, K is a scalar that depends on the shape of crystallites (here we adopt 0.78 as Trabelsi et al. (2003a)), λ is the radiation wavelength, θ is the Bragg angle and $\text{FWHM}_{2\theta}$ is the full width at half maximum of the peak hkl in 2θ. Finally, the disorientation ψ_{hkl} (compared to the mean orientation) of the hkl diffraction plane in the cristallites is simply given by half the full width at half maximum (FWHM_{β}) of the peaks, measured on the azimuthal profiles of the reflection.

3 RESULTS AND DISCUSSION

3.1 *Strain-induced crystallization as revealed by WAXD patterns*

Figure 4 shows the diffraction patterns for filled NR in undeformed state (Fig. 4a), uniaxial tension (Fig. 4b), biaxial tension (Fig. 4c) and equibiaxial tension (Fig. 4d). For each state, the deformation gradient **F** is given. In the undeformed state, the diffraction pattern consists of a diffuse amorphous halo and a ring due to the (100) Bragg reflection of ZnO. Fig. 4b exhibits the diffraction reflections of crystallized NR in uniaxial tension. The diffraction pattern is of course oriented according to the stretching direction (see the white arrows in the figure). The pattern is composed of eight intense crystalline reflection arcs corresponding to the three different crystallographic planes (200), (201) and (120), ten less intense reflection arcs corresponding to the crystallographic planes (121), (202) and (002), a co-existing amorphous halo, the ZnO reflection ring and stearic acid reflection arcs. The diffraction pattern of crystallized NR in biaxial tension (Fig. 4c) is quite similar to the pattern of NR in uniaxial tension. The pattern is also oriented, according to the main direction of traction (direction of the highest stretch ratio). Some diffraction arcs are not observed in the pattern, and all the arcs (corresponding to the planes (002), (201), (200) and (120)) are much less intense and wider. When filled NR is subjected to equibiaxial tension (Fig. 4d), the diffraction pattern is quite different. As previously, an amorphous halo, a ZnO ring and stearic acid arcs are observed. But the diffraction reflections of the NR crystalline phase are rings and not arcs. Only the reflections corresponding to the planes (201) and (200) are visible.

3.2 *The orientation of the crystallites depends on B...*

In order to measure the width of the arcs and ring corresponding to the (201) plane, azimuthal spectra are extracted from the three previous diffraction patterns of NR in deformed state and shown in Figure 5; the Bragg angle 2θ=12.3° corresponds to the position of the (201) arcs and ring in the three patterns. The origin of β is arbitrarily defined as the horizontal direction in the biaxial tension pattern (β=-36° is the tension direction and β=54° is the direction perpendicular to the tension direction for all the tests). The width of the reflection arcs in the patterns (i.e. the width at half maximum of the peaks in the spectra) directly stems for the orientation of the crystallites: the wider the arcs, the more disoriented the crystallites. In the case of equibiaxial loading, the reflections of the planes (200) and (201) are rings which means the crystallites are not oriented in the plane of tension. This result extends those of Oono et al. (1973) who showed that the crystallites are oriented in the direction perpendicular to the traction directions in a thin film of NR. The low anisotropy which can be observed in the spectrum of the equibiaxial test is due to experimental settings (it can also be observed in patterns of amorphous undeformed samples). In the case of uniaxial and biaxial tension, all the reflections of the crystalline phase are arcs, which means that the

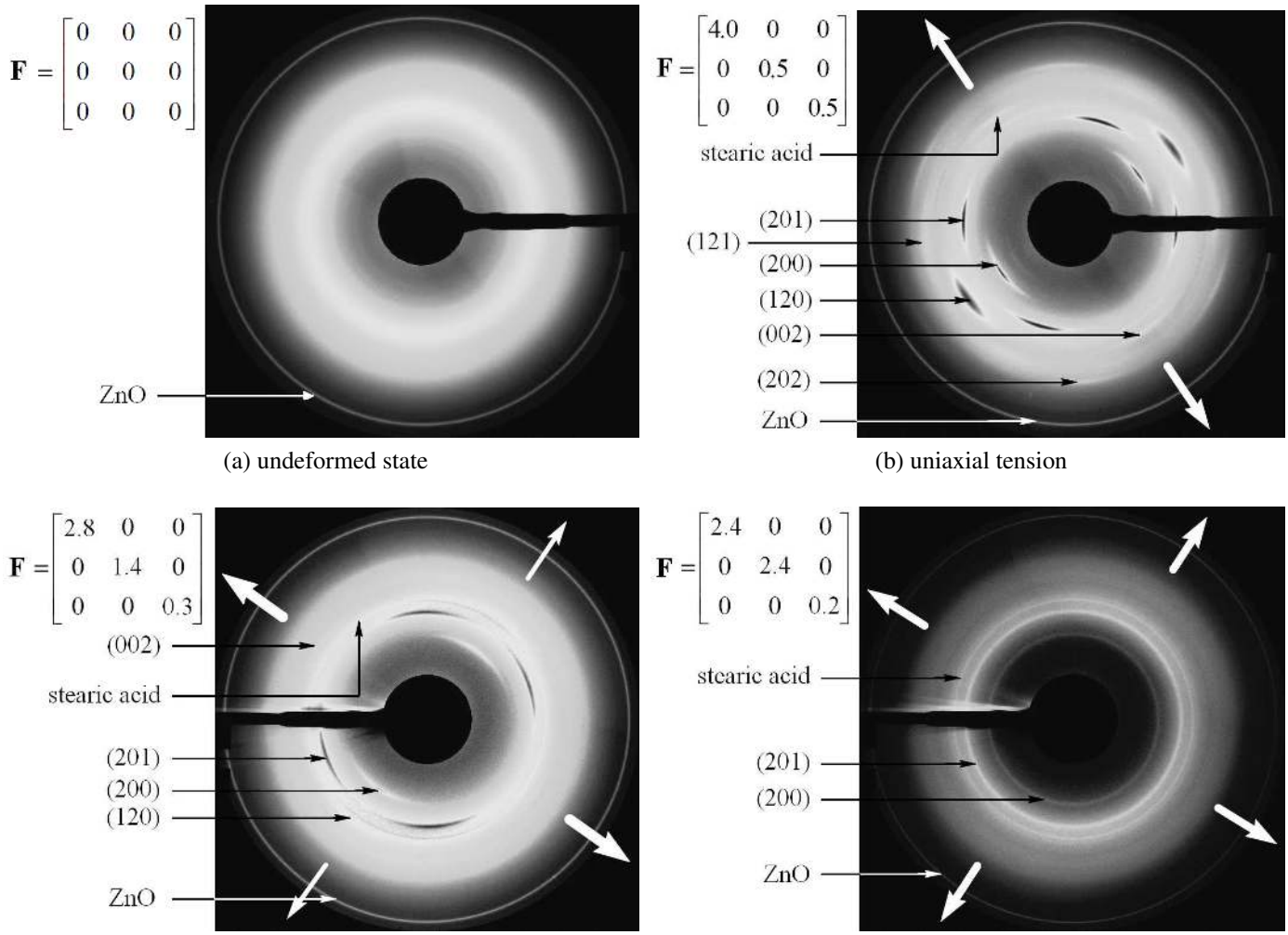

(a) undeformed state (b) uniaxial tension

(c) biaxial tension (d) equibiaxial tension

Figure 4: Scattering patterns of NR in different deformation states (**F** is the deformation gradient; the white arrows show the tensile directions).

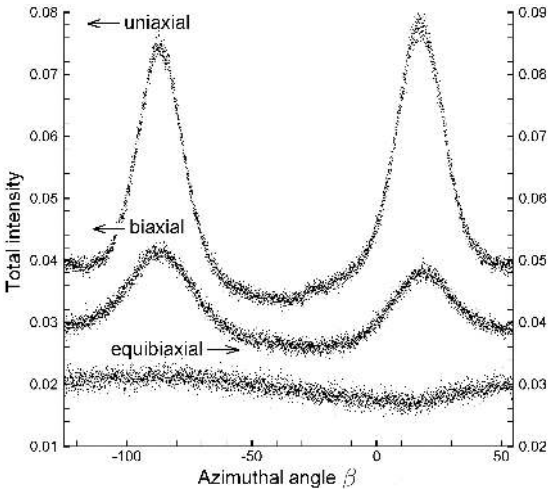

Figure 5: Azimuthal spectra at 2θ=12.3° (Bragg angle of the (201) arcs and ring) for different deformation states: uniaxial tension, biaxial tension and equibiaxial tension.

crystallites are oriented in the plane of tension. Furthermore, the (002) arcs are aligned with the direction of tension for the uniaxial test and with the direction of tension of highest stretch ratio for the biaxial test, which means that the *c*-axis of the crystall cell of the crystallites is in average oriented along the main direction of tension. As the peaks in the spectrum of the biaxial test are wider at half maximum than the peaks in the spectrum of the uniaxial test, the crystallites are more disoriented in NR subjected to biaxial tension than to uniaxial tension. The exact disorientation of the crystallites for each deformation state is measured and given in Table 2, in comparison with the biaxiality factor B. In uniaxial tension, the crystallites are

Table 2: Biaxiality factor and disorientation of the crystallites.

loading conditions	B	$\psi_{200}(^\circ)$	$\psi_{201}(^\circ)$
uniaxial	-0.5	11.70	11.09
biaxial	0.3	15.25	17.03
equibiaxial	1	90	90

disoriented of about 11°; it is slightly smaller than in Poompradub et al. (2005) and twice smaller than in Trabelsi et al. (2003b). This discrepancy is explained by the difference in cross-link densities: indeed, the crystallites orientation highly depends on cross-link density, i.e. formulation and processing, especially for filled NR (Chenal et al. 2007, Poompradub et al. 2005, Tosaka et al. 2004, Trabelsi et al. 2003b, Trabelsi et al. 2003a). Tab. 2 confirms that the disorientation of the crystallites is higher when the material is in biaxial deformation state than when it is in uniaxial deformation state. Furthermore, it suggests that the larger the

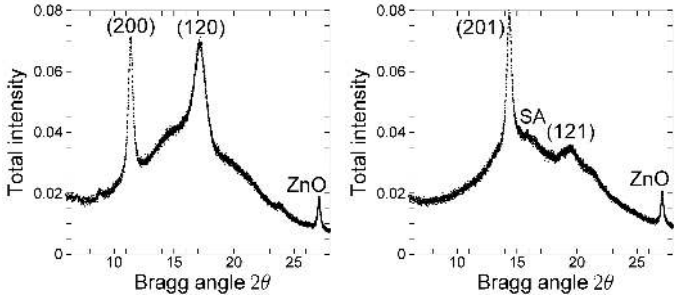

(a) Uniaxial tension - β=54°

(b) Uniaxial tension - β=22°

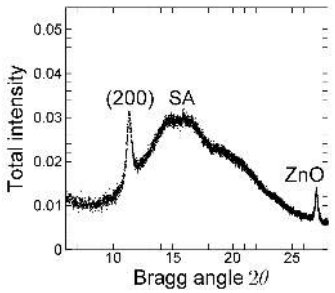

(c) biaxial tension - β=54°

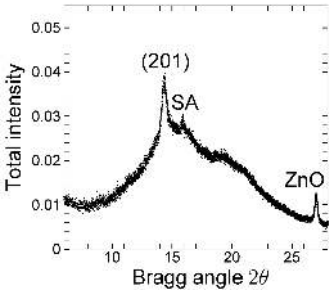

(d) biaxial tension - β=22°

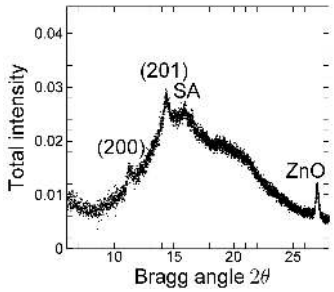

(e) equibiaxial tension - β=22°

Figure 6: Bragg angle spectra for different loading conditions and different azimutal angles β (SA: stearic acid).

biaxiality factor, the higher the disorientation.

3.3 ... *but the crystallites are identical*

The Bragg angle spectra corresponding to the three deformed states are shown in Figure 6: the azimuthal angles are chosen in order to observe the (200) peaks (β=54°, Fig. 6a and 6c) and the (201) peaks (β=22°, Fig. 6b, 6d and 6e). For the equibiaxial tension test, only one spectrum at any azymuthal angle β is necessary to observe both reflections as the pattern is isotropic.

From Fig. 6, we deduce the lattice parameters of the crystal unit cell and the size of the crystallites for the three tests; results are given in Tables 3 and 4 respectively. The crystall cell unit is identical for the three

Table 3: Lattice parameters.

loading conditions	a (Å)	c (Å)
uniaxial	13.38	8.90
biaxial	13.35	8.93
equibiaxial	13.33	9.04

deformation states. Indeed, the diffraction angles of the (200) and (201) planes are very close for the three tests: the corresponding lattice parameters only differ from 1.5% maximum. The lattice parameters of the

Table 4: Size of the crystallites.

loading conditions	l_{200}(Å)	l_{201}(Å)
uniaxial	127.2	121.2
biaxial	135.9	122.1
equibiaxial	122.5	120.7

crystall cell in uniaxial tension are larger than those calculated by other authors in carbon-black filled NR (for example, Poompradub et al. (2004) have found $a = 12.65$ Å, $b = 9.15$ Å and $c = 8.35$ Å). This difference may arise from our calibration method of Bragg angles with the (100) plane ZnO ring. Indeed, the lattice parameter a of the ZnO used for calibration corresponds to pure ZnO, and may slightly differ from the parameter of industrial ZnO inside rubber. This discrepancy with the bibliography does not influence the previous comparative result as the same method has been used for the three tests. This extends the recent result of Poompradub et al. (2004), who demonstrated that the lattice parameters of filled NR only slightly evolve with strain in uniaxial tension: we demonstrate here that they do not change with the deformation state either.

The crystallites sizes obtained for uniaxial tension are quite different from the results obtained in the rare studies published on crystallization of carbon black-filled NR: $l_{200} = 127.2$ Å and $l_{201} = 121.2$ Å, compared to $l_{200} = 170$ Å or $l_{200} = 220$ Å (depending on the quantity of fillers) found by Poompradub et al. (2005) and $l_{002} = 100$ Å found by Trabelsi et al. (2003b). But this discrepancy is explained by the difference in cross-link densities, similarly as the difference in crystallites disorientation. From the results given in Tab. 4, one may conclude that crystallites in NR subjected to uniaxial, biaxial and equibiaxial deformation states have the same size. But we observe in uniaxial tension that crystallites size depends on strain as shown in Table 5; similar results are given in Poompradub et al. (2005) and Tosaka et al. (2004). In

Table 5: Crystallites size in uniaxial tension for different stretch ratios λ.

λ	l_{200}(Å)	l_{201}(Å)
2.8	161	145
3.4	147	137
4.0	127	121

order to precisely compare results in uniaxial, biaxial and equibiaxial tension, it would then be necessary to measure the crystallites size at different stretch ratios in biaxial and equibiaxial deformation states.

4 CONCLUSION

Firstly, this work shows that in equibiaxial tension crystallization of filled NR is isotropic in the plane of tension; it results in rings in the diffraction pattern. It is very different from crystallization in uniaxial tension which is strongly anisotropic, as revealed in the diffraction pattern by narrow reflection arcs. In biaxial (non-equibiaxial) tension, crystallites of filled NR

have an intermediate orientation: they are oriented in average along the direction of highest stretch ratio but the level of disorientation is higher than in uniaxial tension; indeed the reflection arcs in the diffraction pattern are wider for biaxial tension than for uniaxial tension. It seems that the larger the biaxial factor B calculated from the deformation gradient is, the more disoriented crystallites are. Secondly, crystallites are similar in uniaxial, biaxial and equibiaxial deformation states: the lattice parameters of the cristal unit cell are identical and the size of the crystallites is of the same order of magnitude. This result is illustrated in Figure 7.

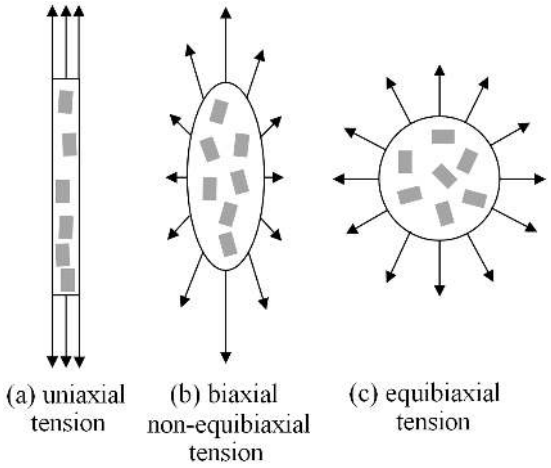

Figure 7: Schematic representation of crystallites in stretched filled NR: the more biaxial the loading conditions are, the more disoriented the crystallites are; but crystallites are identical (in size and lattice parameters) for all experiments.

5 ACKNOWLEDGEMENT

The authors thank Dr D. Thiaudière, Dr C. Mocuta and Dr A. Zozulya from the DiffAbs line in the synchrotron facility Soleil for their great help during the experiments.

REFERENCES

Bunn, C. W. (1942). Molecular structure and rubber-like elasticity i. the crystal structures of beta gutta-percha, rubber and polychloroprene. *Proceedings of the Royal Society of London Series A-Mathematical and Physical Sciences 180(A980)*, 40–66.

Chenal, J.-M., L. Chazeau, L. Guy, Y. Bomal, & C. Gauthier (2007). Molecular weight between physical entanglements in natural rubber: A critical parameter during strain-induced crystallization. *Polymer 48*, 1042–1046.

Chenal, J.-M., C. Gauthier, L. Chazeau, L. Guy, & Y. Bomal (2007). Parameters governing strain induced crystallization in filled natural rubber. *Polymer 48*, 6893–6901.

Demmerle, S. & J. P. Boehler (1993). Optimal design of biaxial tensile cruciform specimens. *Journal of the Mechanics and Physics of Solids 41*, 143–181.

Guinier, A. (1963). *X-ray Diffraction*. W. H. Freeman & Co.

Huneau, B. (2011). Strain-induced crystallization of natural rubber: a review of X-ray diffraction investigations. *Rubber Chemistry And Technology 84*, to appear.

Marckmann, G. & E. Verron (2006). Comparison of hyperelastic models for rubberlike materials. *Rubber Chemistry And Technology 79*, 835–858.

Murakami, S., K. Senoo, S. Toki, & S. Kohjiya (2002). Structural development of natural rubber during uniaxial stretching by in situ wide angle X-ray diffraction using a synchrotron radiation. *Polymer 43*, 2117–2120.

Oono, R., K. Miyasaka, & K. Ishikawa (1973). Crystallization kinetics of biaxially stretched natural rubber. *Journal of Polymer Science 11*, 1477–1488.

Poompradub, S., M. Tosaka, S. Kohjiya, Y. Ikeda, S. Toki, & B. S. Hsiao (2004). Lattice deformation of strain-induced crystallites in carbon-filled natural rubber. *Chemistry Letters 33*, 220–221.

Poompradub, S., M. Tosaka, S. Kohjiya, Y. Ikeda, S. Toki, I. Sics, & B. S. Hsiao (2005). Mechanism of strain-induced crystallization in filled and unfilled natural rubber vulcanizates. *Journal of Applied Physics 97*, 103529/1–103529/9.

Ran, S., D. Fang, X. Zong, B. S. Hsiao, B. Chu, & P. F. Cunniff (2001). Structural changes during deformation of kevlar fibers via on-line synchrotron SAXS/WAXD techniques. *Polymer 42*, 1601–1612.

Rault, J., J. Marchal, P. Judeinstein, & P. A. Albouy (2006). Chain orientation in natural rubber, part II: 2H-NRM study. *The European Physical Journal E 21*, 243–261.

Reeber, R. R. (1970). Lattice parameters of ZnO from 4.2 degrees to 296 degrees K. *Journal of Applied Physics 41*, 5063–5066.

Toki, S., T. Fujimaki, & M. Okuyama (2000). Strain-induced crystallization of natural rubber as detected real-time by wide-angle X-ray diffraction technique. *Polymer 41*, 5423–5429.

Toki, S., I. Sics, S. Ran, L. Liu, & B. S. Hsiao (2003). Molecular orientation and structural development in vulcanized polyisoprene rubbers during uniaxial deformation by in-situ synchrotron X-ray diffraction. *Polymer 44*, 6003–6011.

Toki, S., I. Sics, S. F. Ran, L. Z. Liu, B. S. Hsiao, S. Murakami, K. Senoo, & S. Kohjiya (2002). New insights into structural development in natural rubber during uniaxial deformation by in situ synchrotron X-ray diffraction. *Macromolecules 35*), 6578–6584.

Tosaka, M., S. Murakami, S. Poompradub, S. Kohjiya, Y. Ikeda, S. Toki, I. Sics, & B. S. Hsiao (2004). Orientation and crystallization of natural rubber network as revealed by WAXD using synchrotron radiation. *Macromolecules 37*, 3299–3309.

Trabelsi, S., P. A. Albouy, & J. Rault (2003a). Crystallization and melting processes in vulcanized stretched natural rubber. *Macromolecules 36*, 7624–7639.

Trabelsi, S., P. A. Albouy, & J. Rault (2003b). Effective local deformation in stretched filled rubber. *Macromolecules 36*, 9093–9099.